MULTEQ Simulation for Deposit Formation on Zirconium Oxide with UV Irradiation

Taeho Kim[a,b], Benoit Queylat[b], Ambard Antoine[c], Adrien Couet[b]

[a]Nuclear Fuel Cycle Process Research Division, Korea Atomic Energy Research Institute, 111 Daedeok-daero 989 beon-gil, Yuseong-gu, Daejeon 34057, Republic of Korea.
[b]Department of Engineering Physics, University of Wisconsin-Madison, Madison, WI 53715, USA
[c]EDF Research and Development, Materials and Mechanics of Components, Ecuelles, 77818 Moret-sur-Loing, France

[*]*Corresponding author: tkim@kaeri.re.kr*

1. Introduction

It has been reported that photon (gamma) irradiation may have a significant effect on zirconium alloy corrosion kinetics [1], and there are various photon sources with a wide energy spectrum in the core of a nuclear power plant, from ultraviolet (UV) light, generated by decelerating electrons in water (Cerenkov effect), to gamma from nuclear decays and γ emission. This photon irradiation can influence the corrosion of zirconium alloys by two different mechanisms, one is emergence of photocurrent generated by electron-hole pairs in the oxide itself, and the other is change of corrosion potential due to water radiolysis [2–4], and also it has been reported that the average photon energy from the Cerenkov effect is enough to generate photoelectrons in ZrO_2 (n-type with band gap between 2 and 5 eV) [5]. The differences between predicted weight gain vs measured weight gain from out-of-reactor data is much larger than in-reactor data, supporting the idea that photon (gamma) flux influences the corrosion rate of zirconium alloy. Furthermore, several literatures have been focused on the effect of UV effect on corrosion of zirconium alloy under BWR condition [2,6,7], but the effect of UV irradiation on zirconium alloy under PWR condition is not fully investigated. Therefore, in this study, MULTEQ simulation has been adopted to investigate the mechanism of deposit formation on zirconium oxide with UV irradiation.

2. Experimental

A water circulation loop connected with the autoclave has been developed for the in-situ UV irradiation cell, and it is displayed in Figure 1. The 5 L autoclave is connected to the water circulation loop with high-pressure pump, heat exchanger, and pre-heater. The dissolved oxygen level is maintained below 100 ppb, and dissolved hydrogen concentration is maintained as 2.5 ppm. Zircaloy-4 coupon supplied from Westinghouse is used for this study.

Figure 2 shows the actual cell design with the adaptor, and Zircaloy-4 coupon, and this cell is installed on the wall of the autoclave just in front of the sapphire window. Corrosion experiment has been conducted at 260 °C DI water condition with circulation loop for maintaining water chemistry. MULTEQ version 4.0 developed by EPRI is adopted to simulate how ions dissolved in water can generate deposits on the zirconium oxide with UV irradiation.

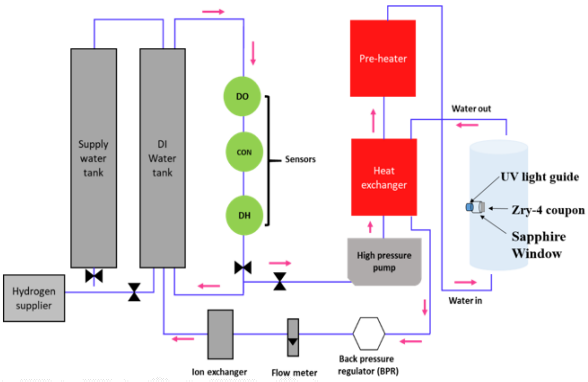

Figure 1. Schematic of the circulation loop connected with the autoclave

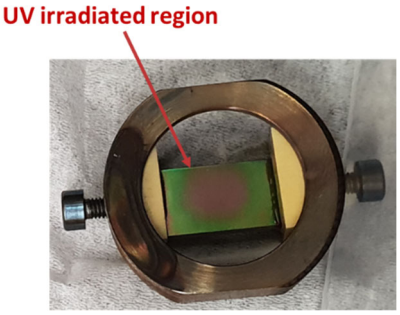

Figure 2. Images of UV irradiated sample at 260 ˚C DI water for 7 days in flowing autoclave

3. Results and Discussion

Table 1 is ICP-OES data obtained after 30 d corrosion in the flowing loop experiment with UV irradiation. This data is used as the input file for MULTEQ simulation. The system temperature is set as 260 °C, and 2592 L of water is considered the total amount water into the autoclave (0.06 mL/min, 30 d). Total numbers of simulation run is set as 8, and the system pH at 260 °C is 6.06. Oxidation potential after run #8 is -0.44 V. Table 2 shows the summary of water chemistry of the system.

Table 1. ICP-OES data obtained after 30 d corrosion flowing loop experiment

	[ppm]	[ppm] / 2592 kg Water
Al	3.70×10^{-3}	9.59
Ca	4.72×10^{-2}	122.39
Cu	5.96×10^{-4}	1.54
Fe	3.85×10^{-2}	99.81
K	3.33×10^{-2}	86.21
Mg	4.90×10^{-2}	126.96
Ni	6.24×10^{-2}	161.74
Zn	1.10×10^{-4}	0.29

Table. 2 Summary of water chemistry of MULTEQ simulation

SUMMARY

Run#	Conc. Factor	pH	Neutral pH	Ionic Strength	Iterations	BP Elev.(°C)	System Temp. (°C):	Steam Fraction	Mass Liquid Water (kg)	Steam Pres. (bar)	Volatile Pres. (bar)	Steam Density (sg)
8	1.00E+00	6.06	5.6	9.80E-06	8	0	260	0.00E+00	1.00E+00	4.69E+01	1.57E-04	2.37E-02

Table. 3 Normalized species disposition from MULTEQ simulation

[Fe+2]

Run Number	FeOH+	Fe(OH)3-	Fe+2	Fe(OH)4-	Fe(OH)2+	FeOH+2	Fe(OH)3	Fe3(OH)4+5	Fe+3	Fe(OH)2	Fe2(OH)2+4
8	1.96	0	4.64	2.65	0	0	80.17	0	0	10.58	0

[Ni]

Run Number	Ni(OH)3	Ni(OH)2	NiOH	Ni	Ni(s)	NiFe5O8(s)	Ni3Fe9O16(s)	NiFe11O16(s)	Ni(OH)2(s)	NiFe2O4(s)	NiO(s)
8	0	0.38	0.85	0.79	0	0	0	0	0	32.37	65.62

Table 4. Amount of species concentration from MULTEQ simulation

Species Conc. (ppm)

Zn(OH)3	Zn(OH)4	CaOH	Cu(OH)2	H	K	Al	Ni(OH)3	OH
8.34E-07	1.29E-11	7.84E-04	5.18E-09	8.76E-04	3.33E-02	7.04E-18	9.73E-09	1.23E-01
Al(OH)2	Ni(OH)2	NiOH	Cu2(OH)2+2	Zn	ZnOH	Al(OH)4	FeOH+	CuOH+
1.69E-08	3.76E-04	6.82E-04	2.99E-19	4.94E-07	4.36E-05	1.30E-02	2.81E-06	7.84E-10
Mg	Zn(OH)2	Cu+2	Al(OH)3	Fe(OH)3-	Ca	Fe+2		
3.05E-02	1.13E-04	1.71E-11	8.35E-08	3.77E-09	4.67E-02	5.09E-06		

From MULTEQ simulation, as shown in Table 2, most Fe is existed as $Fe(OH)_3$ and $Fe(OH)_2$, and Fe ions can also exist, but no Fe metal observed. 5.09 × 10^{-6} ppm (9.73 ppb) of Fe^{2+}, 2.81 × 10-6 ppm $FeOH^{+}$, and 3.77 × 10^{-9} ppm $Fe(OH)^{3-}$ are in the system. It can be concluded Fe is existed as ion or hydroxide form in the solution. Two precipitates are found from MULTEQ simulation, First, NiO(s) = 5.21 × 10-5 g (52.1 μg), $NiFe_2O_4$ = 8.06 × 10-5 g (80.6 μg), and still they are negligible amount.

The total concentration of Fe in the electrolyte is the summation of each Fe species concentration and it is equal to 2.69×10^{-4} ppm. This value is equivalent to 0.269 μg /kg in the solution. From SEM and TEM analysis performed, the deposits are identified as Fe_3O_4 and we will assume an average size of about 2 μm × 2 μm × 2 μm. The total deposit area on the ZrO_2 surface is approximately 1 mm × 1 mm and we will assume that a maximum of 80% of this area is actually covered by the deposits.

An approximate total maximum of 100,000 numbers of deposits are on the surface, corresponding to a total volume of deposit as 8.00×10^{14} nm^3. The density of Fe_3O_4 is 5.17 g/cm^3 corresponding to 5.17×10-21 g/nm^3. Consequently, and under these relatively conservative assumptions, the total mass of Fe_3O_4 on the surface would be about 4.13 μg.

Table 5. Concentration of Fe species in the electrolyte and mass of Fe in the electrolyte (unit: ppm)

	$Fe(OH)_2$	$Fe(OH)^3$	Fe^{2+}	$FeOH^{+}$
Concentration in the electrolyte	4.07 $\times10^{-4}$	3.05 $\times10^{-5}$	1.61 $\times10^{-9}$	2.07 $\times10^{-7}$
Ratio of Fe in the molecule	0.62	0.52	1	0.77
Concentration of Fe in the electrolyte	**2.53 $\times10^{-4}$**	**1.59 $\times10^{-5}$**	**1.61 $\times10^{-9}$**	**1.59 $\times10^{-7}$**

4. Conclusions

The total water volume of the 30 d experiment is 2592 L (considering water flow from high-pressure pump), so the amount of Fe from ICP-OES data and MULTEQ results in 2592 L electrolyte is 697.2 μg. This value is order of magnitudes higher than the mass of Fe from the deposits, which was already an upper estimate based on the assumptions. This clearly shows that Fe ions dissolved in the electrolyte can be the source of Fe_3O_4 on Zr oxide during corrosion with UV irradiation.

REFERENCES

[1] D.M. Rishel, B.F. Kammenzind, The Role of Gamma Radiation on Zircaloy-4 Corrosion, Zircon. Nucl. Ind. 18th Int. Symp. (2018) 555–595.
[2] P. Barberis, M. Skocic, D. Kaczorowski, D. Perche, Y. Wouters, K. Nowotka, Shadow corrosion: Experiments and modeling, J. Nucl. Mater. 523 (2019) 310–319.
[3] H. Gerischer, Electrochemical Behavior of Semiconductors under Illumination, J. Electrochem. Soc. 113 (1966) 1174.
[4] H. Gerischer, On the interpretation of photoelectrochemical experiments with passive layers on metals, Corros. Sci. 31 (1990) 81–88.
[5] M. Inagaki, M. Kanno, H. Maki, Effect of Alloying Elements in Zircaloy on Photo-Electrochemical Characteristics of Zirconium Oxide Films, Zircon. Nucl. Ind. Ninth Int. Symp. (1991) 437.
[6] B. Cox, Some thoughts on the mechanisms of in-reactor corrosion of zirconium alloys, J. Nucl. Mater. 336 (2005) 331–368.
[7] P. Buttin, B. Malki, P. Barberis, B. Baroux, Numerical analysis of the galvanic coupling in the shadow corrosion of zirconium alloy, J. Nucl. Mater. 420 (2012) 591–596.